Supporting Information

Seltmann et al. 10.1073/pnas.1310493110

SI Text

A modified power law, previously described by Maloney et al. (1) in 2010, was used to fit the stretch and relaxation phase of our creep compliance curves:

$$J(\text{stretch}) = At^a + B$$

$$J(\text{relax}) = J(\text{end of stretch}) - Ct^a.$$

The exponent a is used to fit the pooled data of both creep deformation and relaxation. A and C are the amplitudes of the respective stretch and relaxation phase of the modified power law, and B is an offset parameter (1). Whereas a is a measure of the ratio of viscous and elastic contribution, with 1 being perfectly viscous and 0 perfectly elastic, A and C reflect the magnitude of the visco-elastic property. As previously reported, the values of a lie well in the range of 0.1–0.3, and all latrunculin A (LatA)-treated cells show the nearly the same value (Table S1), which is due to their similar curve shape for both the stretch and relaxation phases described in the main text (Fig. 2*B*). The values of B for the offset parameter are confirmed to be negative as reported by Maloney et al.

1. Maloney JM, et al. (2010) Mesenchymal stem cell mechanics from the attached to the suspended state. *Biophys J* 99(8):2479–2487.

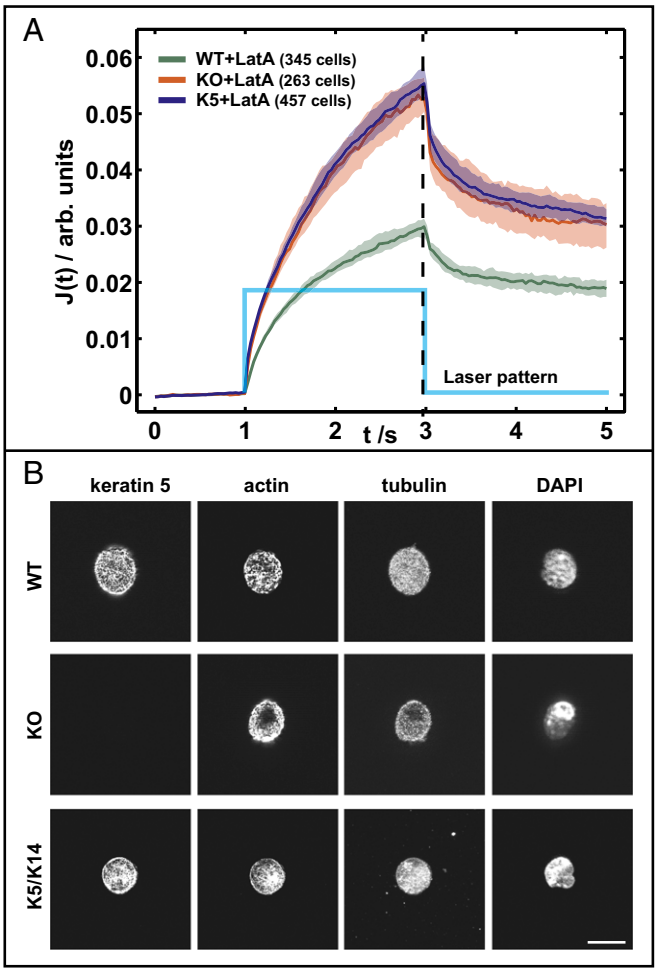

Fig. S1. Creep deformation curves of LatA-treated cells and immunostainings of suspension cells. (*A*) Creep deformation curves $J(t)$ and corresponding 95% CIs for LatA-treated cells (*B*) Immunofluorescence staining of actin (phalloidin), keratin 5, tubulin, and the cell nucleus (DAPI) for spherical cells in suspension.

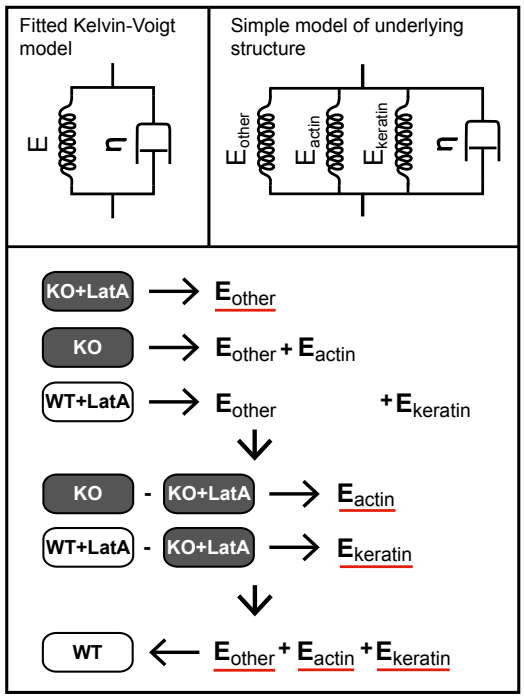

Fig. S2. Simple Kelvin-Voigt based model. The idea of the presented effective values of the simple Kelvin-Voigt model is to give a descriptive idea in terms of elastic values and to support the qualitative discussion in the main text based on the raw data presented concerning the interconnection between the different filament systems inside the cell (Table S1). Obviously it's a simplified model and not suited to appropriately describe a cell as to mention only the deficit that the relaxation phase cannot be well described. However, one could visualize the filament system inside the cell as a parallel circuit of three independent springs, one for each keratin, actin, and other filaments, and an additional viscous element η capturing the fluid properties of the cytoplasm (Fig. S3). The viscosity η was found to be similar for all cell types; thus, the value was set to a constant previously determined by a fit of both elasticity E and viscosity η for all cells. With this simple model, we can test whether the logic presented in the schematic of Fig. S3 holds true. Surprisingly, the simple effective model can be used to estimate the right value for E of untreated WT cells from the E obtained for WT+LatA, KO, and KO+LatA, which can be seen as an additional indication for a low interconnection of the filamentous networks. Relative elastic contribution can accordingly be calculated to $E_{keratin} = 0.421$, $E_{actin} = 0.044$, and $E_{other} = 0.542$.

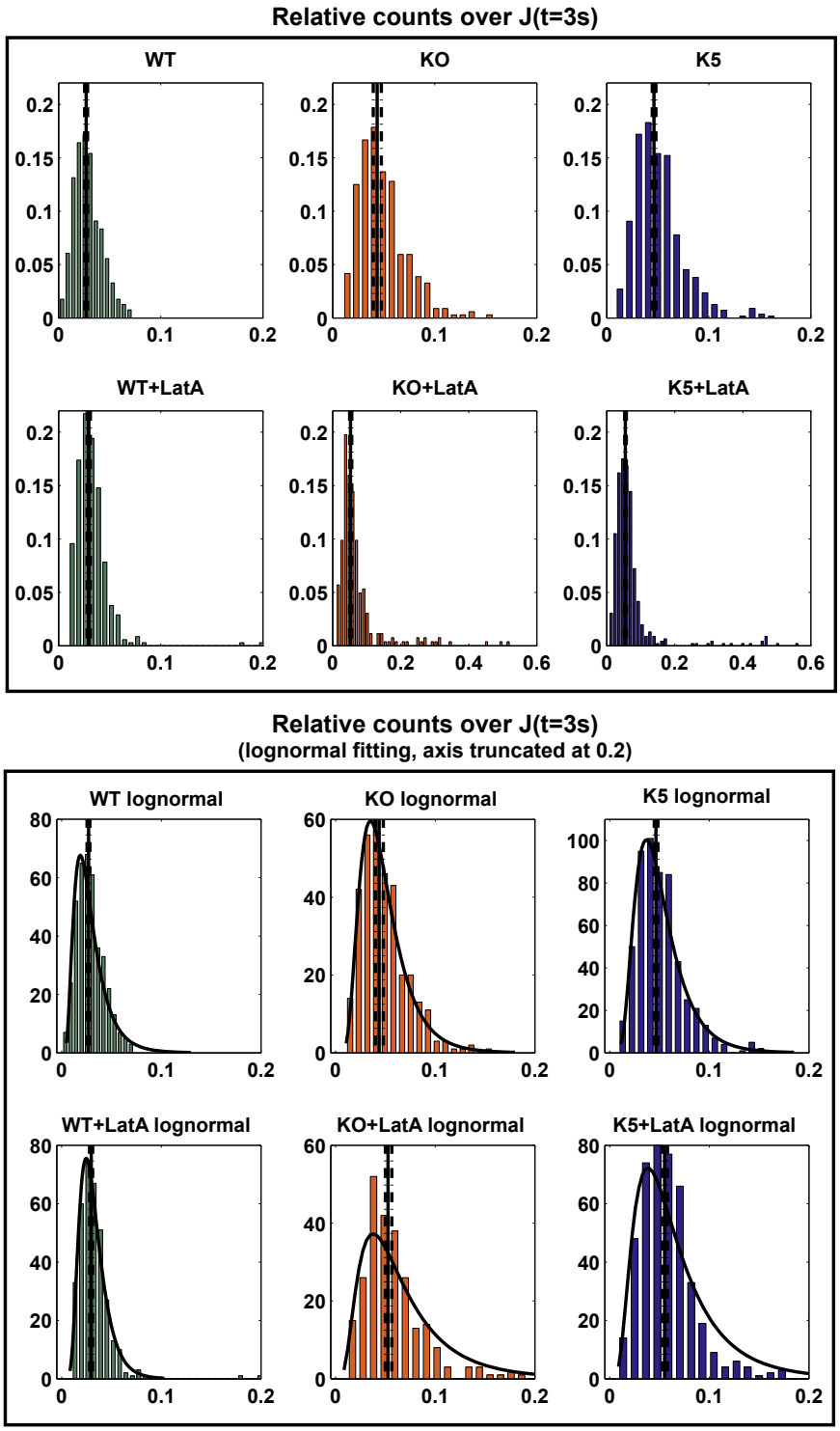

Fig. S3. Distributions of maximal creep deformations. The non-Gaussian distributions of the creep deformations J ($t = 3$ s) and the corresponding median and 95% CIs are displayed for all measurements presented in this work. The lognormal fitting is reasonable for WT, KO, and K5 cells; when treated with LatA, deviations are obvious.

Table S1. Overview of optical stretcher measurements

Variable/parameter	WT	WT+LatA	KO	KO+LatA	K5	K5+LatA
J (t = 3 s)	0.0269	0.0299	0.0434	0.0528	0.0466	0.0553
CI lower	0.0255	0.0279	0.0398	0.0498	0.0447	0.0528
CI upper	0.0283	0.0310	0.0477	0.0562	0.0483	0.0579
E	1.000	0.963	0.586	0.542	0.564	0.509
η	0.395	0.395	0.395	0.395	0.395	0.395
SSR	$3.48E^{-04}$	$3.32E^{-04}$	$6.79E^{-04}$	$6.65E^{-04}$	$6.53E^{-04}$	$6.70E^{-04}$
a	0.103	0.260	0.222	0.259	0.184	0.257
A	0.0645	0.0266	0.0643	0.0482	0.0711	0.0473
B	−0.0439	−0.0095	−0.0361	−0.0203	−0.0419	−0.0177
C	0.0066	0.0070	0.0021	0.0132	0.0039	0.0138
SSR	$1.91E^{-04}$	$8.69E^{-05}$	$3.81E^{-04}$	$2.33E^{-04}$	$3.13E^{-04}$	$1.63E^{-04}$
Cell count	396	345	336	263	552	457

Median creep deformation values at the end of the stretch phase J (t = 3 s) as presented in the main text figures and their corresponding CIs calculated via the bootstrapping method. Median ensemble elasticity E and viscosity η values derived via a Kelvin-Voigt model fit of the stretching phase and normalized to the median elasticity E of the WT cell ensemble. Median ensemble values a, A, B, and C of a modified power law, previously described by Maloney et al. in 2010, are derived from fits to the pooled data of the stretch and relaxation phases of our creep deformation curves. The median ensemble values of the sum of squared residuals (SSR) are presented for both models as a measure of fit quality.

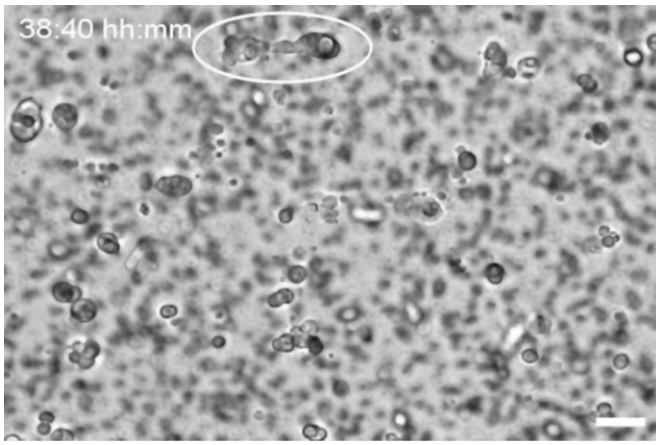

Movie S1. Time-lapse images of WT cells on a Boyden chamber. To monitor WT, KO, and K5 cells during invasion, they were recorded on top of the transwell Bodyen chamber. Here, additionally to the invasion behavior displayed in Fig. 3, we see the fusion of cells to colonies and cells leaving them to invade. For KO cells, a higher number of single cells leaving the large colony from finger-like protrusions and a faster migration can be seen. In contrast, WT and K5 keratinocytes colonies stay compact and have tendencies to fuse to larger colonies. (Scale bar, 100 μm.)

Movie S1

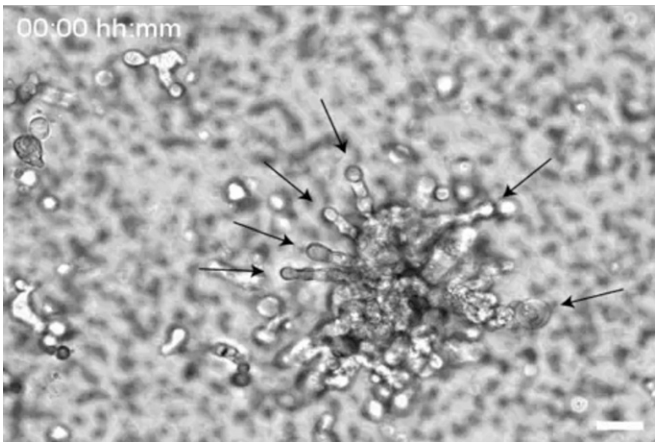

Movie S2. Time-lapse images of KO cells on a Boyden chamber. To monitor WT, KO, and K5 cells during invasion, they were recorded on top of the transwell Bodyen chamber. Here, additionally to the invasion behavior displayed in Fig. 3, we see the fusion of cells to colonies and cells leaving them to invade. For KO cells, a higher number of single cells leaving the large colony from finger-like protrusions and a faster migration can be seen. In contrast, WT and K5 keratinocytes colonies stay compact and have tendencies to fuse to larger colonies. (Scale bar, 100 μm.)

Movie S2

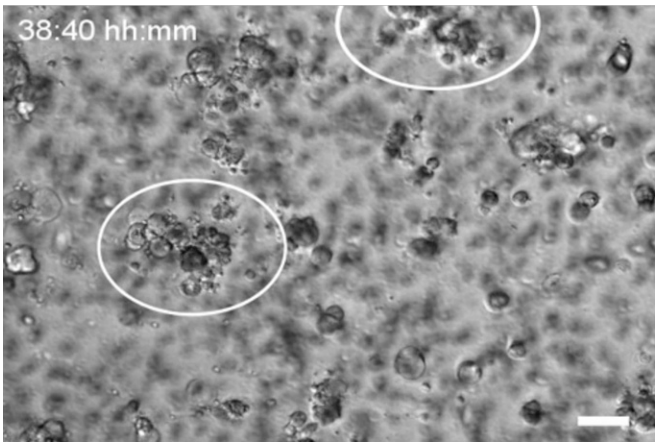

Movie S3. Time-lapse images of K5 cells on a Boyden chamber. To monitor WT, KO, and K5 cells during invasion, they were recorded on top of the transwell Bodyen chamber. Here, additionally to the invasion behavior displayed in Fig. 3, we see the fusion of cells to colonies and cells leaving them to invade. For KO cells, a higher number of single cells leaving the large colony from finger-like protrusions and a faster migration can be seen. In contrast, WT and K5 keratinocytes colonies stay compact and have tendencies to fuse to larger colonies. (Scale bar, 100 μm.)

Movie S3